Energy Proceedings
Vol 51, 2025
ISSN 2004-2965

A Novel Power Generation Model for Bifacial Photovoltaic Modules Based on Parallel Equivalent Circuits#

Qiangzhi Zhang [1], Jinqing Peng[1,2*], Yimo Luo[1,2**]

1 College of Civil Engineering, Hunan University, Changsha, 410082, Hunan, China

2 Key Laboratory of Building Safety and Energy Efficiency of Ministry of Education, Hunan University, Changsha, Hunan, China
(Corresponding Author: jqpeng@hnu.edu.cn, yimoluo@hnu.edu.cn)

ABSTRACT

Using a static bifaciality to simulate the dynamic output power of bifacial photovoltaic (bPV) modules would produce errors. To address the problem, the present study proposed a novel parallel equivalent circuit model based on the single diode model, incorporating the structural characteristics and electrical properties of bPV modules. The results showed that the difference between the novel model and the traditional model increased as irradiance decreasing. When the incident solar irradiance on the module was 100 W/m², the output power simulated by the novel model is 3.3% lower than that of the traditional model and is more aligned with actual conditions. Further analysis showed that the difference between the two models increased with module temperature, though temperature changes have less impact than solar irradiance changes. Additionally, there is a superimposed effect between module temperature and irradiance. When the module temperature is 60°C and the irradiance is 100 W/m², which significantly differs from the standard test conditions (STC), the simulation results of the novel model are 4.3% lower than those of the traditional model.

Keywords: bifacial photovoltaic, power generation, five parameters model, parallel equivalent circuit

NONMENCLATURE

Abbreviations	
PV	photovoltaic
bPV	bifacial photovoltaic
mPV	monofacial photovoltaic
LCOE	levelized cost of energy
EVA	ethylene-vinyl acetate copolymer
MPP	maximum power point
STC	standard test conditions
Symbols	
I_{sc}	short-circuit current (A)
V_{oc}	open-circuit voltage (V)
I_{mp}	current at MPP (A)
V_{mp}	voltage at MPP (V)
α	temperature coefficient of I_{sc} (%/℃)
β	temperature coefficient of V_{oc} (%/℃)
γ	temperature coefficient of P_{max}(%/℃)
I_{ph}	photo-generated current (A)
I_0	reverse saturation current (A)
R_s	series resistance (Ω)
R_p	parallel resistance (Ω)
V_t	thermal voltage of the diode (V)
q_e	electron charge (1.6×10^{-19} C)
E_g	band gap (eV)
K_0	Boltzmann's constant (1.38×10^{-23} J/K)
G	Irradiance intensity(W/m^2)
Subscripts	
f	front side
r	rear side

1. INTRODUCTION

Bifacial photovoltaic modules (bPV) can generate electricity by absorbing solar energy from both sides[1,2]. Compared to traditional monofacial photovoltaic (mPV) modules, bPV offer higher power output per unit area and can reduce the levelized cost of electricity (LCOE)[3], which makes them more competitive in the market. In 2022, the global market share of bPV cells was 65%, while bPV modules held a market share of 30%. By 2033, the market share of bPV cells was expected to reach 90%, and the market share of bPV modules was projected to reach 70%[4].

To effectively deploy bPV systems, it is essential to develop an accurate bPV power generation model. Currently, static bifaciality measured under STC (1000 W/m², module temperature 25°C, AM1.5 spectrum) is commonly used to simulate the output power of bPV

This is a paper for the 16th International Conference on Applied Energy (ICAE2024), Sep. 1-5, 2024, Niigata, Japan.

modules [5] . However, the actual operating conditions of bPV modules largely differ from STC. Experimental studies have shown that the bifaciality is not a constant value. It is influenced by solar irradiance intensity and increases with higher irradiance[6–8]. Therefore, using a static bifaciality to simulate the dynamic output power of bPV modules in actual operation often leads to overestimated results. Based on this, this study proposed a parallel equivalent circuit model on the foundation of the single-diode model by incorporating the structural characteristics and electrical properties of bPV modules. This model could accurately simulate the dynamic output power of bPV modules by considering the impact of solar irradiance intensity on the electrical performance of the module's front and rear sides.

The paper is organized as follows. Section 2 introduced the structure of bPV modules and the electrical performance parameters under STC. Section 3 introduced the single-diode model and the developed parallel equivalent circuit model for bPV modules based on it. Section 4 compared the simulated output power of the bPV module under different conditions using traditional methods and the newly proposed method. Section 5 summarized the key conclusions of the paper.

2. SYSTEM DESCRIPTION

As shown in *Fig. 1*, the bPV module consists of five layers: upper glass, upper ethylene-vinyl acetate copolymer (EVA), bifacial photovoltaic cell, lower EVA, and lower glass. This study used a monocrystalline silicon bPV module, with the nameplate parameters provided by the photovoltaic supplier being listed in Table 1.

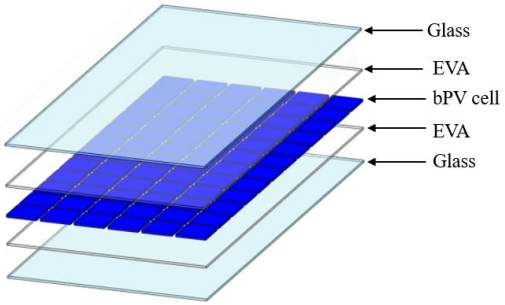

Fig. 1 System structure configuration

Table 1 Electrical parameters of bPV module under STC[9]

Parameters	Front side	Rear side
Short-Circuit Current (I_{sc})	9.96 A	8.53 A
Open-Circuit Voltage (V_{oc})	44.5 V	44.1 V
Voltage at MPP (V_{mp})	37.9 V	37.7V
Current at MPP (I_{mp})	9.38 A	8.00 A
Maximum Power (P_{max})	355 W	302 W
Temperature coefficient of I_{sc}(α)	0.048 %/℃	
Temperature coefficient of V_{oc}(β)	-0.30%/℃	
Temperature coefficient of P_{max}(γ)	-0.38%/℃	

3. METHODOLOGY

3.1 The single-diode model

The output power of PV modules is typically calculated with a single diode model. This model strikes a good balance between simplicity and accuracy in modeling, with its equivalent circuit shown in *Fig. 2*. The circuit consists of four components: a current source, a diode, a parallel resistance, and a series resistance. The relationship between current and voltage in the PV module can be expressed by Eq. (1)[10,11]:

$$I = I_{ph} - I_d - I_p = I_{ph} - I_0\left[\exp\left(\frac{V+I\cdot R_s}{V_t}\right) - 1\right] - \frac{V+I\cdot R_s}{R_p} \quad (1)$$

Where I_{ph} is the photo-generated current, I_d is diode current, I_p is the current flowing through the parallel resistance, I_0 is the reverse saturation current of the diode, R_s is the series resistance, R_p is the parallel resistance, V_t is the thermal voltage of the diode.

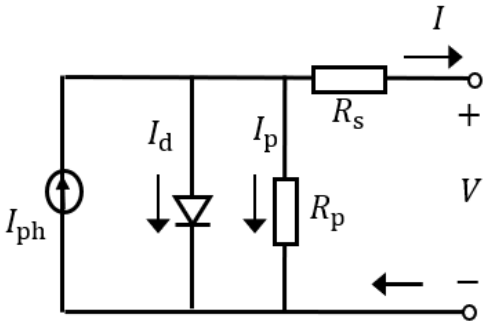

Fig. 2 Equivalent circuit of the single diode model

I_{ph}, I_0, R_s, R_p, and V_t are the five unknown parameters in Eq. (1). By substituting the parameters from the PV module's nameplate into Eq. (1), the five parameters under STC can be determined: $I_{ph,stc}$, $I_{0,stc}$, $R_{s,stc}$, $R_{p,stc}$, and $V_{t,stc}$[11].

The five parameters are affected by the actual temperature T_{pv} and the actual solar irradiance G_{pv}. Eq. (2) can convert the five parameters under STC to their values under actual operating conditions [12]:

$$\begin{cases} I_{\mathrm{ph}} = \frac{G_{\mathrm{pv}}}{G_{\mathrm{stc}}}(I_{\mathrm{ph,stc}} + \alpha(T_{\mathrm{pv}} - T_{\mathrm{stc}})) \\ I_0 = I_{0,\mathrm{stc}}(\frac{T_{\mathrm{pv}}}{T_{\mathrm{stc}}})^3 \cdot \exp\left[\frac{q_e E_g}{K_0}(\frac{1}{T_{\mathrm{stc}}} - \frac{1}{T_{\mathrm{pv}}})\right] \\ R_s = \frac{T_{pv}}{T_{stc}}(1 - 0.217 \cdot ln\frac{G_{pv}}{G_{stc}})R_{s,stc} \\ R_{\mathrm{p}} = \frac{G_{\mathrm{stc}}}{G_{\mathrm{pv}}}R_{\mathrm{p,stc}} \\ V_{\mathrm{t}} = \frac{T_{\mathrm{pv}}}{T_{\mathrm{stc}}}V_{\mathrm{t,stc}} \end{cases} \quad (2)$$

Where G_{stc} is the solar irradiance under STC (1000 W/m²), T_{stc} is the module temperature under STC

(25°C), α is the temperature coefficient of short-circuit current, q_e is the electron charge (1.6×10^{-19} C), E_g is the energy band gap, and K_0 is the Boltzmann's constant (1.38×10^{-23} J/K).

By substituting the five parameters under actual operating conditions into Eq. (1) to obtain the I-V characteristic equation under the actual operating conditions, the output power of the PV module can be calculated.

3.2 The parallel equivalent circuit model of the bifacial module

As illustrated in *Fig.* 3(a), the schematic structure of a bPV cell shows that when exposes to sunlight, light transmits through the anti-reflection coatings from both sides of the cell. Photons with energy greater than the bandgap of the bPV cell are utilized for PV generation. Considering the structural characteristics of bPV cells and that the total photo-generated current of bPV cells is the sum of the front and rear photo-generated currents, it can be assumed that the front and rear sides of the bPV cell are in a parallel relationship. The equivalent circuit is shown in *Fig.* 3(b). In this diagram, the red box represents the circuit of the front side of the module, the orange box represents the rear side. Based on this parallel equivalent circuit, Eq. (3) can be derived:

$$I = I_f + I_r \tag{3}$$

Where I_f is output current of the front side of the bPV module, I_r is output current of the rear side of the bPV module.

Referring to Eqs. (1) and (3), the current-voltage relationship of bPV modules can be expressed by Eq. (4):

$$\begin{aligned} I &= \left(I_{ph,f} - I_{d,f} - I_{p,f}\right) + \left(I_{ph,r} - I_{d,r} - I_{p,r}\right) \\ &= I_{ph,f} - I_{0,f}\left[\exp\left(\frac{V + I_f \cdot R_{s,f}}{V_{t,f}}\right) - 1\right] - \frac{V + I_f \cdot R_{s,f}}{R_{p,f}} + \\ &\quad I_{ph,r} - I_{0,r}\left[\exp\left(\frac{V + I_r \cdot R_{s,r}}{V_{t,r}}\right) - 1\right] - \frac{V + I_r \cdot R_{s,r}}{R_{p,r}} \end{aligned} \tag{4}$$

Where the subscripts "f" and "r" denote the front and rear sides of the bPV module, respectively.

By substituting the characteristic parameters of the front and rear sides from the bPV module's nameplate into Eq. (1), the five parameters under STC for both the front and rear sides can be determined. Using Eq. (2), the five parameters for the front side ($I_{ph,f}$, $I_{0,f}$, $R_{s,f}$, $R_{p,f}$, and $V_{t,f}$) and rear side ($I_{ph,r}$, $I_{0,r}$, $R_{s,r}$, $R_{p,r}$, and $V_{t,r}$) under actual operating conditions can then be calculated. Substituting these parameters into Eq. (4) provides the I-V characteristic equation for the bPV module under actual operating conditions.

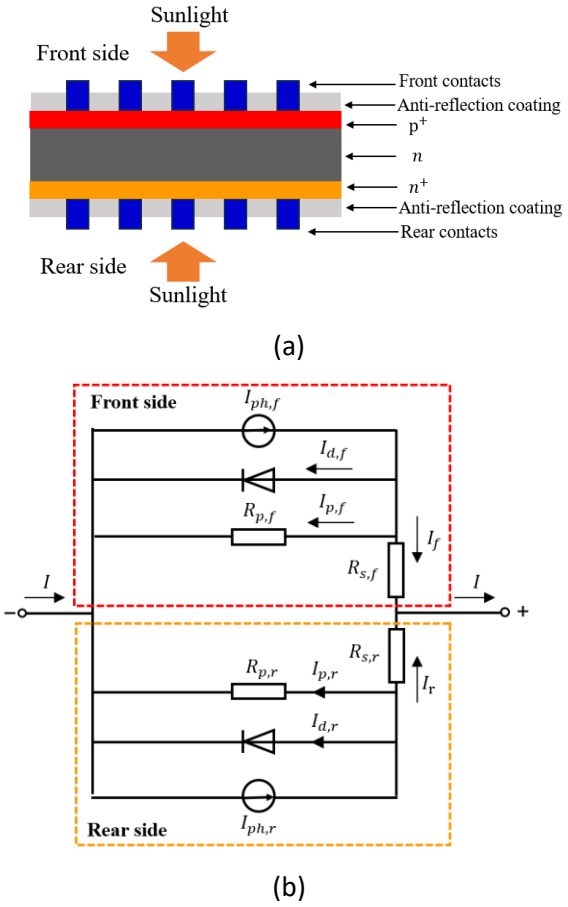

Fig. 3 The structure and equivalent circuit of bPV cell:(a) Structure; (b) *Equivalent circuit.*

4. RESULTS AND DISCUSSION

The main content of this section is to compare the power generation of bPV modules simulated by the newly proposed parallel equivalent circuit model and the traditional static bifaciality model under different conditions.

Fig. 4 shows the I-V characteristics curves of the bPV module simulated with two methods under different irradiance conditions. In Fig. 4(a), both the front and rear irradiance intensities of the bPV module are 1000 W/m². The traditional method has an output power of 662.5 W, while the novel method has an output power of 657.0 W, which is 0.84% lower than the traditional method. When the irradiance intensity decreases to 700 W/m² (Fig. 4(b)), the traditional method has an output power of 455.4 W, while the novel method has an output power of 462.7 W, 1.6% lower than the traditional method. As the irradiance intensity further decreases, the difference between the simulation results of the two methods gradually increases. When the irradiance intensity

decreases to 400 W/m² and 100 W/m² (Figs. 4(c) and 4(d)), the novel method's results are 2.4% and 3.3% lower than those of the traditional method, respectively. In fact, when the irradiance decreases, the bifaciality decreases as well [6–8]. However, traditional methods still use the bifaciality under STC for simulation, leading to an overestimation of power generation with low irradiance conditions. The greater the difference between the irradiance conditions and STC, the larger the relative error between the simulated results and the actual values. It was found that the results of the novel model are lower than those of traditional methods and their difference gradually increases as irradiance decreases, which is consistent with the tendency under the actual condition. Therefore, it was concluded that the novel model could improve the simulation accuracy compared to the traditional methods.

Fig. 5 shows the simulated output power of the bPV module using two methods under different temperature conditions. In Fig. 5(a), with a front and rear side irradiance of 1000 W/m², the output power of the module at 25°C, 30°C, 40°C, 50°C, and 60°C is as follows: 657.0 W, 643.8 W, 617.1 W, 590.1 W, and 563.3 W for the traditional method; and 662.5 W, 649.4 W, 623.3 W, 596.9 W, and 570.2 W for the novel method. Compared to the traditional method, the output power of the novel method is 0.84%, 0.89%, 1.01%, 1.16%, and 1.28% lower at different temperatures. This indicates that higher temperatures increase the deviation of the module's actual operating conditions from the STC, thereby enlarging the discrepancy between the simulation results of the two methods. However, compared to changes in irradiance, the impact of temperature is relatively smaller.

Fig. 5(b) shows the simulated output power of the bPV module using the two methods at different temperatures under a front and rear side irradiance of 100 W/m². As the temperature increases, the discrepancy between the simulation results of the two methods gradually widens. Compared to the differences of simulation results at the same temperature in Fig. 5(a), Fig. 5(b) shows a more pronounced discrepancy between the two methods due to the larger deviation of irradiance from the STC. Particularly at 60°C, where both irradiance and temperature conditions significantly deviate from STC, the simulated output power of the bPV module using the traditional method is 4.3% higher than that by using the novel method. This difference is attributed to the combined effects of both irradiance and temperature.

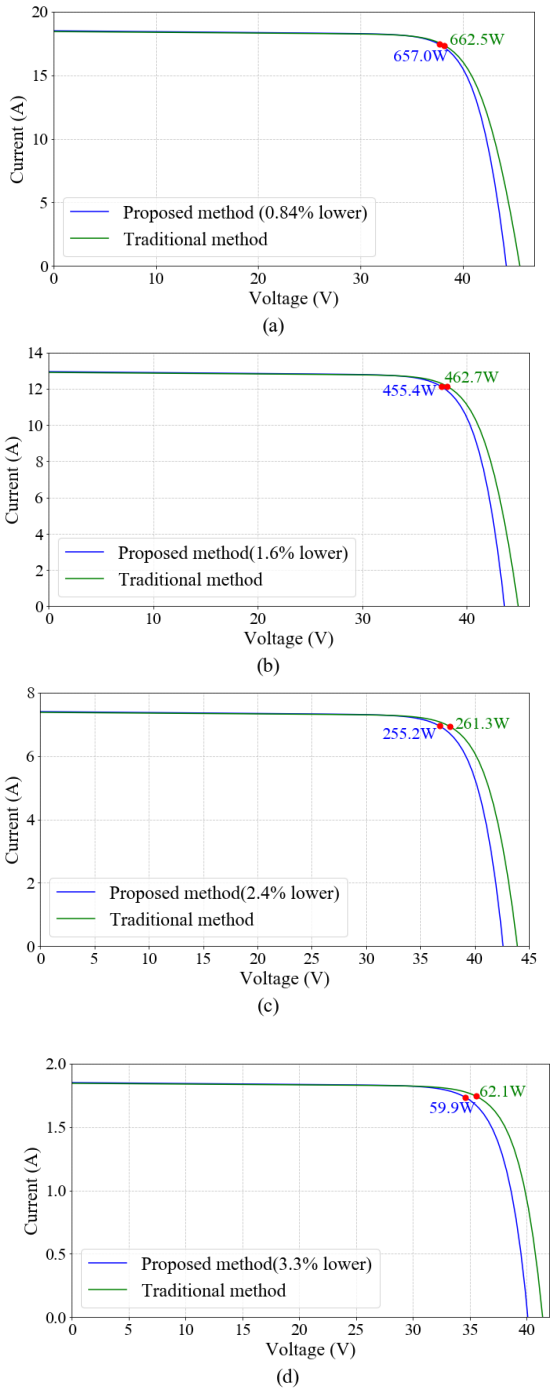

Fig. 4 Comparison of I-V characteristics curves simulated by two methods under different irradiance conditions: (a) G_f = G_r =1000 W/m²; (b) G_f = G_r =700 W/m²;(c) G_f=G_r=400 W/m²; (d) G_f=G_r=100 W/m².

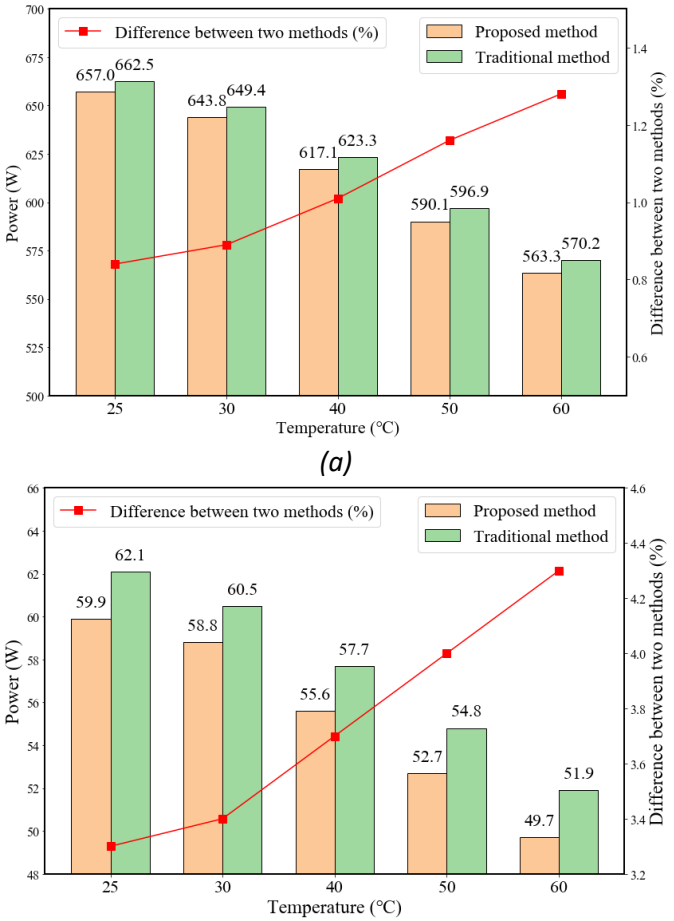

Fig. 5 The output power of the bPV module under different temperatures: (a) $G_f = G_r$ =1000 W/m²; (b) G_f=G_r=100 W/m².

5. CONCLUSIONS

This study proposed a novel parallel equivalent circuit model for bPV modules' power simulation to address the overestimation problem with the traditional methods which adopting a static bifaciality. The results indicated that compared to the traditional model, the power output results of the novel model are lower, which are aligned better with actual conditions. The main conclusions are as follows:

1) By comparing the output power of the two models under different irradiance conditions, it was found that the lower the irradiance conditions, the greater the difference between the simulation results of the novel model and the traditional model. When the irradiance intensity on the front and rear sides of the module is 100 W/m², the power output simulated by the novel model is 3.3% lower than that of the traditional model.

2) As the module temperature increasing, the discrepancy between the simulation results of the novel method and the traditional method also increases. However, compared to changes in irradiance, temperature variations have a smaller impact on the differences between the simulation results of the two methods.

3) The difference of simulation results between the two methods due to the module temperature and the irradiance intensity has a cumulative effect. When the module temperature is 60°C and the irradiance intensity is 100 W/m², the simulated power output by the novel model is 4.3% lower than that of the traditional model.

ACKNOWLEDGEMENT

The study was supported by the National Key R&D Program of China (Grant No.2022YFB4201002) and the Hunan Provincial Science and Technology Department (Grant No. 2021RC3042).

REFERENCE

[1] Eguren J, Martínez-Moreno F, Merodio P, Lorenzo E. First bifacial PV modules early 1983. Solar Energy 2022;243:327–35. https://doi.org/10.1016/j.solener.2022.08.002.

[2] Muehleisen W, Loeschnig J, Feichtner M, Burgers AR, Bende EE, Zamini S, et al. Energy yield measurement of an elevated PV system on a white flat roof and a performance comparison of monofacial and bifacial modules. Renewable Energy 2021;170:613–9. https://doi.org/10.1016/j.renene.2021.02.015.

[3] Patel MT, Khan MR, Sun X, Alam MA. A worldwide cost-based design and optimization of tilted bifacial solar farms. Applied Energy 2019;247:467–79. https://doi.org/10.1016/j.apenergy.2019.03.150.

[4] International technology roadmap for photovoltaic (ITRPV). Results 2022:1–81.

[5] International Electrotechnical Commission. Photovoltaic Devices - Part 1-2: Measurement of Current-Voltage Characteristics of Bifacial Photovoltaic (PV) Devices, IEC TS 60904-1-2 ,2019. n.d.

[6] Sahu PK, Batzelis EI, Roy JN, Chakraborty C. Irradiance Effect on the Bifaciality Factors of Bifacial PV Modules. 2022 IEEE 1st Industrial Electronics Society Annual On-Line Conference (ONCON), Kharagpur, India: IEEE; 2022, p. 1–6. https://doi.org/10.1109/ONCON56984.2022.10126623.

[7] Muñoz-Cerón E, Moreno-Buesa S, Leloux J, Aguilera J, Moser D. Evaluation of the bifaciality coefficient of bifacial photovoltaic modules under real operating conditions. Journal of Cleaner Production

2024;434:139807. https://doi.org/10.1016/j.jclepro.2023.139807.
[8] Bai Q, Tian H, Nan C, Ouyang L, Zhang Y, Ma J, et al. Investigation on bifaciality factor and ideality factor of PERC bifacial solar module under different irradiances. 2021 IEEE 48th Photovoltaic Specialists Conference (PVSC), Fort Lauderdale, FL, USA: IEEE; 2021, p. 0248–51. https://doi.org/10.1109/PVSC43889.2021.9518575.
[9] Gu W, Ma T, Li M, Shen L, Zhang Y. A coupled optical-electrical-thermal model of the bifacial photovoltaic module. Applied Energy 2020;258:114075. https://doi.org/10.1016/j.apenergy.2019.114075.
[10] Celik AN, Acikgoz N. Modelling and experimental verification of the operating current of mono-crystalline photovoltaic modules using four- and five-parameter models. Applied Energy 2007;84:1–15. https://doi.org/10.1016/j.apenergy.2006.04.007.
[11] De Soto W, Klein SA, Beckman WA. Improvement and validation of a model for photovoltaic array performance. Solar Energy 2006;80:78–88. https://doi.org/10.1016/j.solener.2005.06.010.
[12] Xiong W, Liu Z, Wu Z, Wu J, Su F, Zhang L. Investigation of the effect of Inter-Building Effect on the performance of semi-transparent PV glazing system. Energy 2022;245:123160. https://doi.org/10.1016/j.energy.2022.123160.